



# Machinability of wood fiber/polyethylene composite during orthogonal cutting

Xiaolei Guo<sup>1</sup> · Jinxin Wang<sup>1</sup> · Dietrich Buck<sup>2</sup> · Zhaolong Zhu<sup>3</sup> · Yong Guo<sup>4</sup>

Received: 22 June 2020 / Accepted: 14 December 2020 / Published online: 4 January 2021  
© The Author(s), under exclusive licence to Springer-Verlag GmbH, DE part of Springer Nature 2021

## Abstract

Wood fiber/polyethylene composite (WFPEC) is composed of a natural wood fiber and a recyclable polyethylene plastic, which is normally used as an environmental protection composite material. However, better knowledge of chip formation and surface damage mechanism of WFPEC is essential to improve its machinability for extending exterior and interior applications. In this article, machinability of WFPEC was investigated by analyzing the disparity between cutting efficiency and surface quality through a group of orthogonal cutting experiments with change of cutting depth. The chip formation process was recorded by a high-speed camera system with 5000 frames per second. Surface topography was observed by a scanning electron microscope. The results showed that the chip morphology changed from continuous cutting governed by a continuous shearing process under the shallow cutting depth, to a discontinuous cutting governed by plastic fracture under the deep cutting depth ahead of the tool tip. Flattened matrix was the main form of surface topography caused by shallow cutting depth, while matrix-fiber tearing was caused by deep cutting depth. Pullout/fracture and debonding of fibers were related to the fiber orientation angle and the diameter of fiber bundles, but not to the cutting depth. Taken together, the toughness of the workpiece material in the cutting region decreased with the increase in cutting depth. To avoid matrix-fiber tearing, shallow cutting depth should be used during finishing to maintain surface quality. In contrast, pre-cutting can be performed with a deep cutting depth in order to improve the cutting efficiency.

---

✉ Xiaolei Guo  
xiaolei.guo@njfu.edu.cn

- <sup>1</sup> College of Materials Science and Engineering, Nanjing Forestry University, No. 159 Longpan Road, Nanjing, Jiangsu, China
- <sup>2</sup> Division of Wood Science and Engineering, Luleå University of Technology, Skellefteå, Sweden
- <sup>3</sup> College of Furnishings and Industrial Design, Nanjing Forestry University, Nanjing, China
- <sup>4</sup> College of Forest and Garden, Anhui Agricultural University, Hefei, China

## Introduction

Wood fiber/polyethylene composite (WFPEC) is an environmentally friendly material composed of a natural wood fiber and a recyclable polyethylene plastic (Kilinc et al. 2019). WFPEC, as a member of wood plastic composite (WPC), has attracted significant attention due to its durability in response to fire, weather, and biological attack in many exterior and interior applications, such as parts in automobiles, buildings, decking, fencing, highway construction, and many others (Bazant et al. 2014; Fowler et al. 2006; Lin and Renneckar 2011; Pelaez-Samaniego et al. 2013).

Many applications have specific requirements for size and accuracy of WFPEC. To meet these requirements for dimension, shape, and surface roughness, secondary processing of WFPEC such as milling, sawing, drilling, and grinding is critical (Saloni et al. 2011; Thibaut et al. 2016).

In practical production, there is always a disparity between production efficiency and surface quality that needs to be solved. Increasing cutting depth is an economical and effective way to improve productivity. However, great differences in cutting depth have a significant influence on the surface quality of the product (Gao et al. 2019). For example, the machinability of wood flour/polyvinyl chloride composite was investigated by Guo et al. (2015). They concluded that the machined surface roughness increases with the increase in cutting depth. However, they did not provide an explanation of the surface damage mechanism with different cutting depths.

Orthogonal cutting, which is still a basic method of cutting mechanism research, is suitable to analyze most problems related to chip formation and surface quality (Wyeth et al. 2009). A review on the progress of WPC cutting indicates that it is of great significance to study the surface quality of the machined surface by analyzing the chip formation mechanism (Wei et al. 2018). For wood-based materials, the chip formation mechanism has been reported to be mainly due to plastic shearing (Nairn 2016), which is greatly different from monolithic metallic, adiabatic shear localization or crack initiation, and propagation (Davis et al. 2017; Komanduri and Von Turkovich 1981; Vyas and Shaw 1999). Although the effect of cutting depth on chip morphology of wood flour/ polyvinyl chloride composite, wood flour/polyethylene composite, and wood flour/polypropylene composite has been reported (Guo et al. 2014), the authors did not reveal the mechanisms of chip formation, which is essential to improve machinability of WPC (Kuzu and Bakkal 2016).

The machinability of WPC depends not only on cutting parameters, but also on the size and form of the dispersed phase used in their preparation (Madhavan et al. 2015). WPC is composed of a dispersed phase consisting of wood flour or wood fiber as the filler, and a continuous phase consisting of plastics as the matrix. Wood flour consists of hardwood, softwood, or different mixtures of both. The size and form of particles have important effects on the potential damage to the machined surface, which is mainly caused by the extraction of wood flour particles and fracture of the matrix. In contrast, the use of fiber as filler has thus far not been analyzed as regards machinability of wood fiber/plastic composites. Therefore, it is critical to expand the knowledge of machinability of wood fiber/plastic composites to improve production.

This study addresses this gap in knowledge by investigating the machinability of WFPEC under different cutting depths during orthogonal cutting, and quantifying cutting force, chip formation, and surface quality. The aim of this work was to improve the machinability of WFPEC and provide guidance for the WFPEC machining industry.

## Materials and methods

### Materials

WFPEC, supplied by Guofeng Wood Plastic Composite Co., Ltd., (Anhui, China), was subjected to orthogonal cutting. The test workpieces were 120 mm by 60 mm with a thickness of 4 mm. They contained 48 wt.% pine (*Pinus sylvestris* L.) wood fibers, 34 wt.% polyethylene, and 13 wt.% talc, as well as some additives such as lubricants and pigments. The physical and mechanical properties of the WFPEC workpieces are presented in Table 1.

Polycrystalline diamond (PCD) tools were used in cutting experiments due to their outstanding advantages, such as high hardness, low friction coefficient, and high thermal conductivity (Adamovskyi and Kostenko 2019; Chowdhury et al. 2005). The tool had a matrix of high-speed steel with PCD blades welded on it in this test. PCD tools were supplied by Leitz Tooling System Co., Ltd. The average edge radius measured by an optical microscope (SZX16, Olympus, Co., Ltd., Tokyo, Japan) was about 10  $\mu\text{m}$ . The geometry and mechanical properties are described in Table 2.

### Experimental design

The experiments on orthogonal cutting of WFPEC were carried out on a planer (B665, Hefei University of Technology, Anhui, China) with a fixed cutting speed ( $V=13.6$  m/min) and cutting width ( $b=4.0$  mm). The machine was stopped when the tool cuts through the workpiece and back to the starting point. The tool was then

**Table 1** Physical and mechanical properties of the WFPEC

Flexural strength (MPa)	Tensile strength (MPa)	Elasticity strength (MPa)	Impact strength (MPa)	Density ( $\text{kg}\cdot\text{cm}^{-3}$ )	Moisture content (%)
4.69	26.21	$4.27 \times 10^3$	$15.7 \times 10^3$	1.65	14.9

**Table 2** Geometry and physical parameters of the cutting tool

Blade	Angle geometries			Material properties			
	Rake angle ( $^\circ$ )	Wedge angle ( $^\circ$ )	Clearance angle ( $^\circ$ )	Density ( $\text{kg m}^{-3}$ )	Hardness (HV)	Modulus of elasticity (MPa)	Thermal conductivity ( $\text{W m}^{-1} \text{K}^{-1}$ )
PCD	31	47	12	4110	8000	$8 \times 10^5$	560

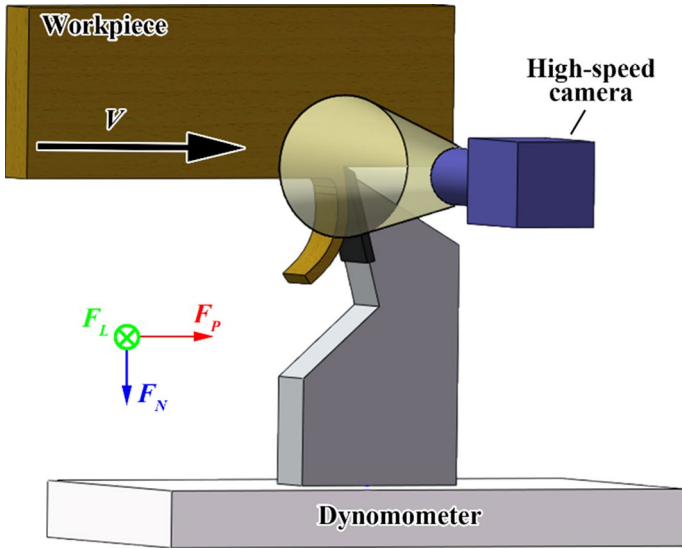


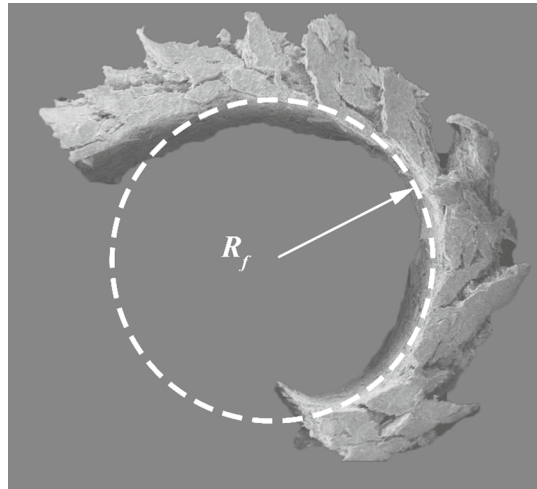
**Fig. 1** Schematic of cutting force measuring and the position of the high-speed camera

lowered by a certain distance to achieve the intended cutting depth by rotating the hand wheel, and the test was repeated five times. Dynamic cutting force was monitored by a dynamometer (Kistler 9257B, Winterthur, Switzerland) with a charge amplifier (5070A, Winterthur, Switzerland) (Fig. 1). The sampling frequency was 7142 Hz, which was higher than the natural frequency (3.5 kHz) of the dynamometer. Three force components in orthogonal cutting ( $F_P$ ,  $F_N$ ,  $F_L$ ) were measured, namely parallel cutting force, normal cutting force, and lateral cutting force, respectively.  $F_L$  was a lateral force, which was not recorded in this test. The cutting parameter was mainly focused on the variable of the cutting depth ( $h$ ): shallow and deep cutting depth. Shallow cutting depth ranged from 0.1 to 0.5 mm at intervals of 0.2 mm, while deep cutting depth ranged from 1.0 to 2.0 mm at intervals of 0.5 mm.

## Characterization

In this study, the chip formation of WFPEC during machining with different cutting depths was investigated via high-speed camera of 5000 frames per second (I-speed 3, Olympus, Co. Ltd., Tokyo, Japan). A scanning electron microscope (SEM) was used to observe the chip morphology. The radius of chip curvature, as a method to evaluate chip deformation, was measured by SEM. An example of the measured radius of chip curvature is shown in Fig. 2. The arithmetic mean deviation  $Ra$  was used to evaluate the roughness of the machined surface by a surface topography profilometer (DSX510, Olympus, Co., Ltd., Japan). The cutoff and sampling lengths for each measurement were set as 2.5 and 13 mm, respectively. The surface roughness  $Ra$  and surface morphology of the machined surface were used as the indexes to evaluate the quality of the machined surface.

**Fig. 2** Radius of the chip curvature at a cutting depth of 1.0 mm



## Results

### Cutting forces

Figure 3 shows the cutting depth achieved with average parallel cutting force and normal cutting force. Both parallel cutting force and normal cutting force initially showed a slight upward trend as cutting depth increases. Due to the

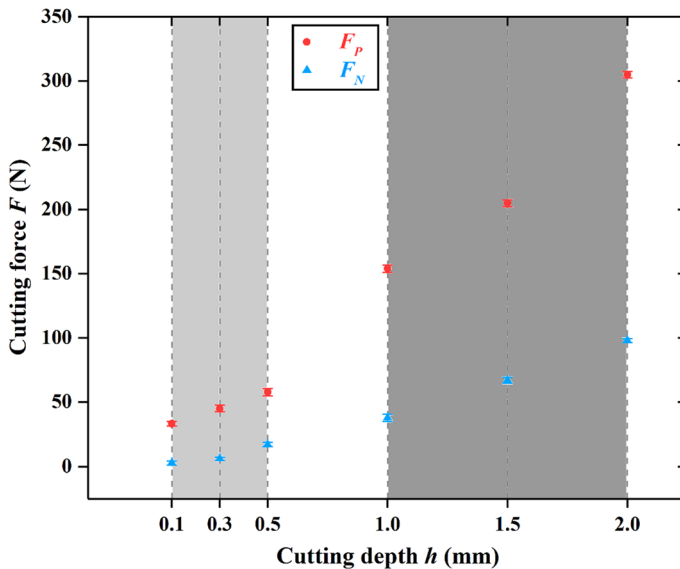


**Fig. 3** Average parallel and normal cutting force as a function of cutting depth. Gray shading indicates the different cutting depths in shallow (light gray) and deep (dark gray) layers of the material

initial interval of cutting depth of 0.2 mm in the shallow layer of the material, the increase in cutting force is slight. When the cutting depth continued to increase, the increase in material removal volume resulted in an increase in cutting forces. When the cutting depth increased to 1.0 mm, both parallel and normal cutting forces increased significantly due to the increase in cutting depth intervals from 0.2 to 0.5 mm, which increased the material removal volume significantly. When the cutting depth reached 2.0 mm, both components showed the highest values. In general, both parallel and normal cutting forces rose with the increase in cutting depth.

### Chip morphology

The chip morphology obtained from different cutting depths during machining WFPEC is shown in Fig. 4. At shallow cutting depths (Fig. 4a–c), spiral-type chips were generated. At a cutting depth of 0.1 mm, the chips sheared under the pushing action of the rake face, and the shear stress did not exceed shear failure strength. Therefore, there were few cracks observed in the chip, and the chip was long and continuous at a cutting depth of 0.1 mm (Fig. 4a). At a cutting depth of 0.3 mm, cracks were regularly distributed on the outer circumference of the chip. This was also observed at the microscopic level in SEM analysis (Fig. 5a). This phenomenon is believed to be caused by the fracture initiation and propagation just ahead of the tool tip (Thibaut et al. 2016). When machining WFPEC at a cutting depth of 1.0 mm, periodic fracture ahead of the tool tip occurred, forming short serrate-type chips. Toughness fracture instead of brittle fracture contributed to the serrate-type chips due to the connected free surface. When the cutting depth reached 2.0 mm, serrate-type chips had a trend of turning into fragmented chips. Separation of serrated nodes was observed at the microscopic level in SEM images (Fig. 5b). Generally, the chips formed at deep cutting depths were shorter and more discontinuous than these at shallow cutting depths.

### Surface roughness

The values of surface roughness ( $R_a$  and  $R_z$ ) under different cutting depths are presented in Fig. 6. Both  $R_a$  and  $R_z$  initially showed a slight increase as cutting depth increases. When the cutting depth increased from 0.5 to 1.0 mm, the mean value of  $R_a$  and  $R_z$  increased significantly by 1.2 and 6.9 mm, respectively. Thus, the surface roughness of WFPEC was more affected by deep cutting depth than by shallow cutting depth, most likely related to the observed change in chip morphology from continuous to fragmented.

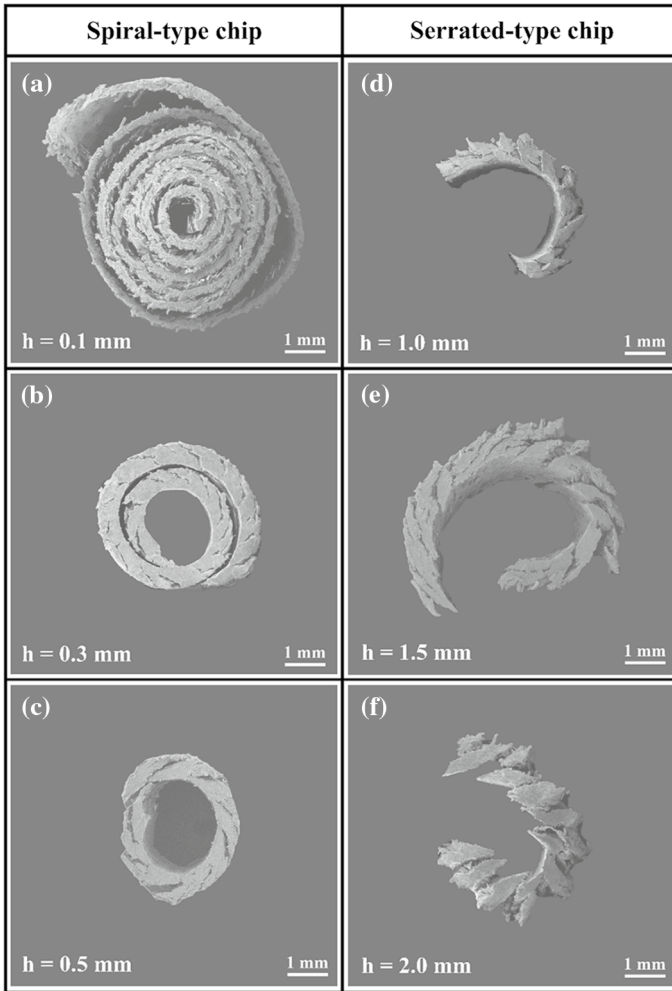
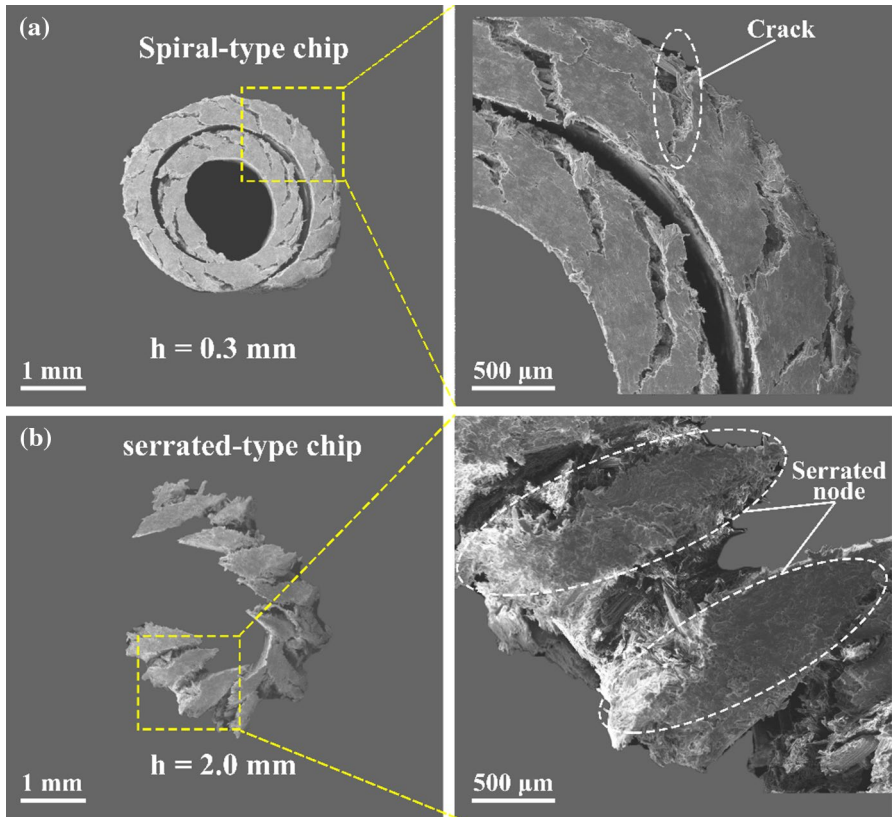


Fig. 4 Chip morphology at different cutting depths

## Discussion

### Chip formation

To investigate chip deformation, the chip formation process was recorded utilizing a high-speed camera. During the stable cutting process, a periodic cutting force signal was observed (Fig. 7a, b). Two typical shapes of chips, continuous, and discontinuous are shown in Fig. 7c, d. The observed periodic cutting force signals were related to the periodic cracks. When cracks happened, the cutting force decreased sharply and then increased again when the cutting conditions were ready for a new circle (Thibaut 1988). Therefore, when the crack is as deep as the chip thickness, the chip



**Fig. 5** Two typical types of chip morphology in shallow and deep cutting depth. **a** Spiral-type chip with cracks distributed on the outer circumference, **b** serrate-type chip with nearly detached serrated nodes

appears discontinuous. As shown in Table 3, in a chip of 10 mm length, the number of cracks with 1.0 mm cutting depth was three times greater than at 0.1 mm cutting depth. This implies that the cutting force signals at 0.1 mm cutting depth had higher frequency than at 1.0 mm cutting depth. Please note that the dynamics of the dynamometer also led to the presence of high frequency components in the cutting force signal. These high frequency components were removed according to a published method (Bachrathy and Stepan 2017). Therefore, these data suggested that the formation of spiral-type chips had less force variations than serrate-type chips and could easily transform into continuous chips.

Figure 8 shows the radius of chip curvature in response to cutting depth. Initially, the chip radius showed a sharp increase with shallow cutting depth. Subsequently, chip radius increased more slowly with incremental increase in cutting depth. Cutting depth and radius of chip curvature showed a positive correlation. It has to be noted that the radii of spiral-type chips were smaller than the radii of serrate-type chips, which indicated that the spiral-type chips governed by continuous shearing had a higher chip formation level than serrate-type chips governed by plastic



fracture. It is likely that the propagation of cracks in chips consumed a high amount of surface generation energy, which likely decreased the surface quality.

## Surface quality

SEM imaging was utilized to assess the topography of the machined surfaces of WFPEC. Surface defects (i.e., pit holes and tears) were observed with different cutting depths (Fig. 9). Pit holes were observed due to compressed PE, pullout/fracture, and debonding of fibers (Fig. 9a). These surface defects were observed to a lesser degree at a cutting depth of 2.0 mm (Fig. 9b) because the cracks below the machined surface were pushed by the rake face of the tool, resulting in surface tearing.

During the formation of spiral-type chips, compressed PE, pullout/fracture, and debonding of fibers were the three main surface defects observed. First, debonding of fibers was usually observed in a diameter range of 40–180  $\mu\text{m}$  regardless of the cutting depth (shallow or deep). When small diameter wood fibers are aggregated into large wood bundles, their specific surface area is much smaller than that of individual fibers before aggregation. Therefore, the main reason for debonding of fibers relates to the reduced bonding strength between wood fiber bundles and PE after aggregation, which results in easier removal by the mechanical movement of the cutter. Secondly, the pullout/fracture of fibers is likely related to the fiber orientation angle regardless of the cutting depth. Similar defects were also presented in the work by Madhavan et al. (2015) when machining carbon fiber-reinforced plastic. They observed occurrence of pullout/fracture of fibers when the fiber orientation

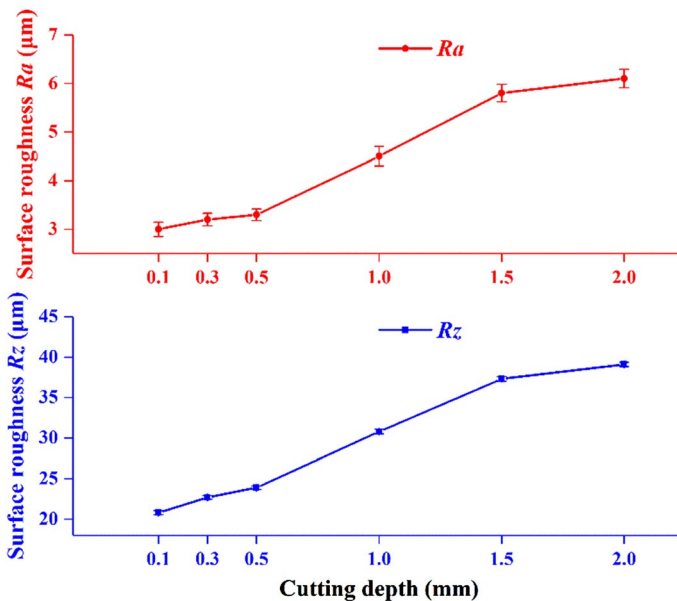
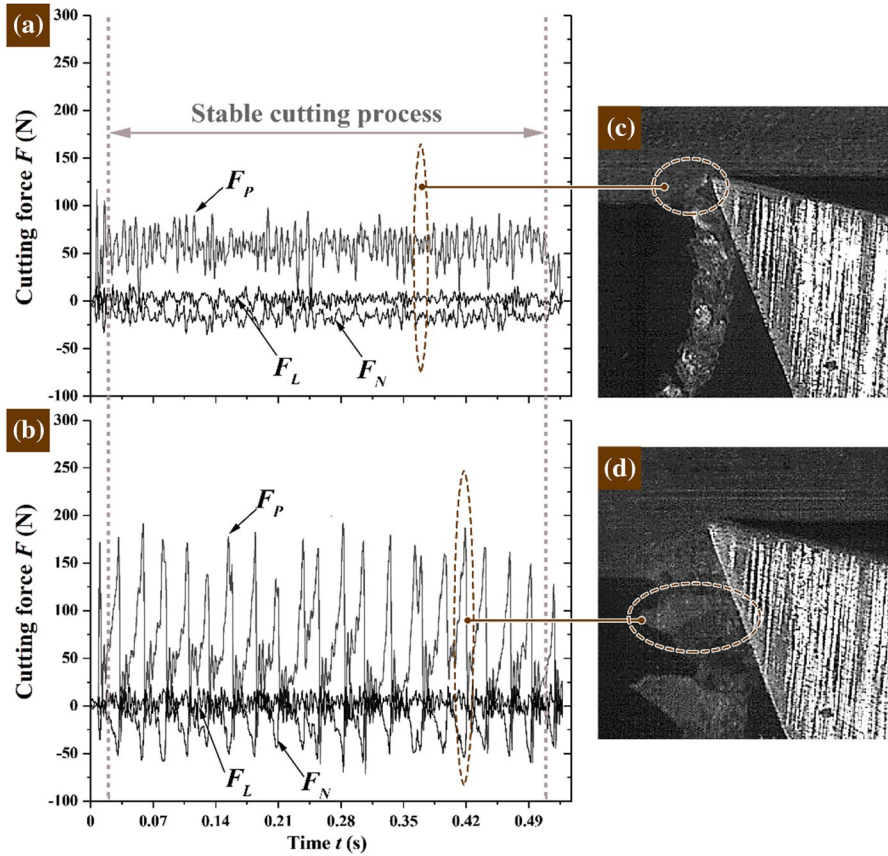


Fig. 6 Effect of cutting depth on surface roughness ( $R_a$  and  $R_z$ )



**Fig. 7** Cutting force signals in shallow and deep cutting depth. **a**  $h=0.1$  mm, **b**  $h=1.0$  mm. During the stable cutting process, two typical types of a continuous and a discontinuous chip are shown in panels (c) and (d), respectively

**Table 3** Number of cracks in a chip of 10 mm length

Cutting depth (mm)	0.1	0.3	0.5	1.0	1.5	2.0
Number of cracks	92	51	34	30	20	11

angle was  $65^{\circ}$ – $80^{\circ}$ . Thirdly, compressed PE was observed with shallow cutting depth. Under the mechanical movement of the cutter, plastic deformation was the main form of chip deformation in the cutting region due to the greater toughness under shallow cutting depth. PE had greater plasticity than fibers and was easier to

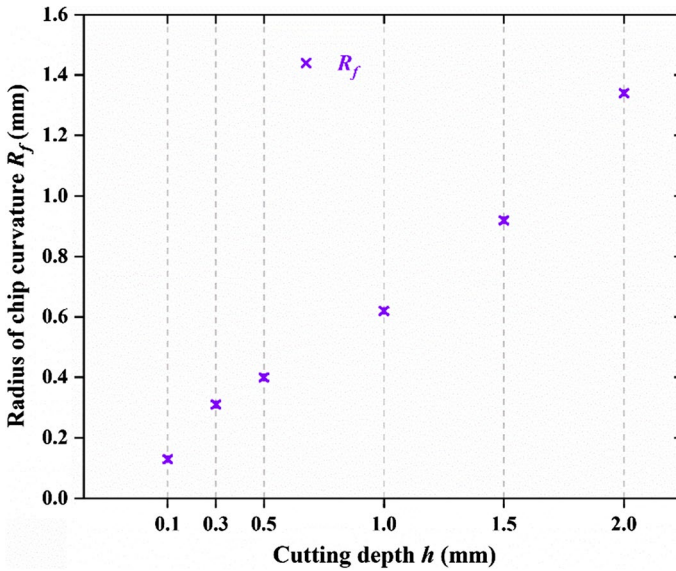


**Fig. 8** Radius of chip curvature as a function of cutting depth

be compressed by the clearance face of the tool. In general, the surface roughness of such pit holes formed by compressed PE, pullout/fracture, and debonding of fibers is relatively low. The defects caused by the structure of WFPEC, such as fiber orientation angle and diameter of fiber bundles, are more significant than these caused by the cutting depth.

During the formation of serrate-type chips, matrix-fiber tearing was a more significant surface defect compared to pit holes. Plastic fracture was the main form of chip deformation in the cutting region. The increase in the cutting forces exceeded the shearing strength of WFPEC under deep cutting depth, and cracks propagated ahead of the tool tip. However, cracks did not propagate instantaneously due to the toughness of WFPEC. Under severe cutting condition ( $h=2.0$  mm), cracks might partly extend below the machined surface, resulting in matrix-fiber tearing under the rake face. The appearance of matrix-fiber tearing is the main reason causing the rapidly increasing surface roughness in the cutting region.

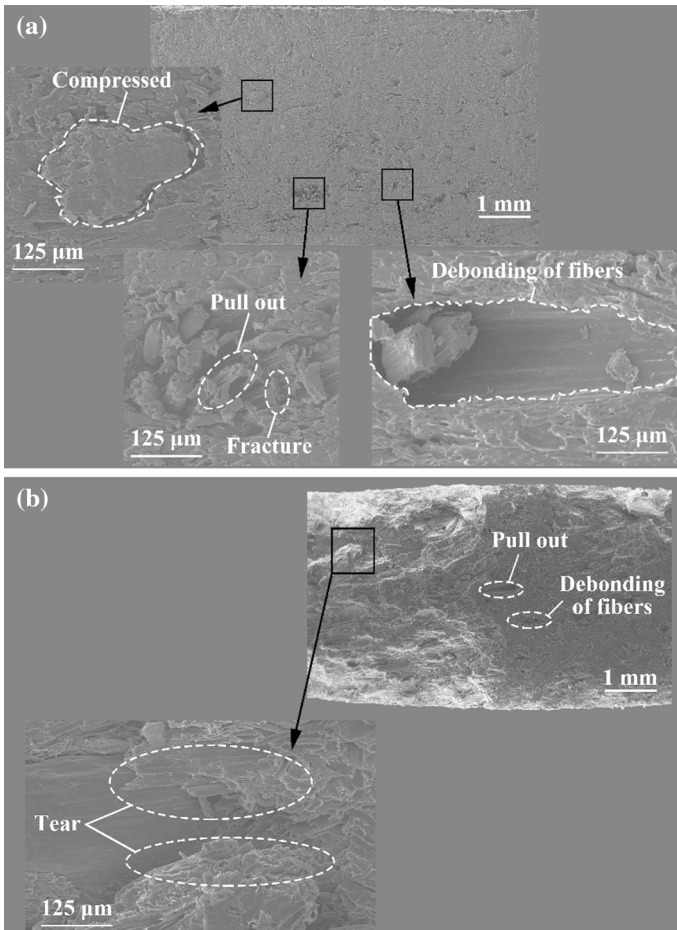


**Fig. 9** Comparison of surface damage in shallow and deep cutting depths. **a**  $h = 0.3$  mm, **b**  $h = 2.0$  mm

## Conclusion

Machinability of WFPEC is greatly affected by the cutting depth during orthogonal cutting. Specifically, large differences were observed in cutting force, chip formation, and surface quality.

Reducing the cutting depth can greatly decrease the fluctuation of cutting forces. It was confirmed that the fluctuation of cutting forces and the chip formation mechanism are closely related, and fracture in chips is a significant source of the fluctuation of cutting forces.

Analysis of the mechanism of chip formation in WFPEC at different cutting depths showed that the toughness of workpiece material in the cutting region decreased with the increase in cutting depth. Chips obtained at a shallow cutting depth were essentially continuous and curly.

The comparison of machined surfaces of WFPEC demonstrates that severe defects appear at deep cutting depths, while at shallow cutting depths, the machined surface is of higher quality. These data suggest that a shallow cutting depth should be used in finishing to maintain surface quality. However, for pre-cutting purposes, deep cutting depth can be used to improve the cutting efficiency.

**Acknowledgements** The authors are grateful for the support from the National Science Foundation of China (31971594), Leitz Tooling System Co., Ltd., for supplying the samples of PCD tools, and Guofeng Wood Plastic Composite Co., Ltd., for supplying the samples of wood fiber/polyethylene composite.

**Authors' contributions** Xiaolei Guo contributed to project administration, experimental design, analysis and discussion of the data, and writing the paper. Jinxin Wang was involved in laboratory experiments, data collection, analysis and discussion of the data, and editing the paper. Dietrich Buck contributed to laboratory experiments, data collection, and review of the paper. Zhaolong Zhu was involved in laboratory experiments, data collection, and supervision of the work. Yong Guo contributed to experimental design, laboratory experiments, and supervision of the work.

**Funding** This study was funded by the National Natural Science Foundation of China (31971594).

**Code availability** Not applicable.

## Compliance with ethical standards

**Conflict of interest** The authors declare that they have no conflict of interest.

**Availability of data and material (data transparency)** The datasets generated and analyzed during the current study are available from the corresponding author on request.

## References

- Adamovskiy AA, Kostenko AD (2019) The friction coefficient of natural diamond against materials based on cubic boron nitride. *J Superhard Mater* 41:281–282
- Bachrathy D, Stepan G (2017) Cutting force measurements in high speed milling: extension of the frequency range of Kistler dynamometer. In: Proceedings of the 39th international MATADOR conference on advanced manufacturing, No. 0033
- Bazant P, Munster L, Machovsky M, Sedlak J, Pastorek M, Kozakova Z, Kuritka I (2014) Wood flour modified by hierarchical Ag/ZnO as potential filler for wood–plastic composites with enhanced surface antibacterial performance. *Ind Crops Prod* 62:179–187. <https://doi.org/10.1016/j.indcr op.2014.08.028>
- Chowdhury S, de Barra E, Laugier MT (2005) Hardness measurement of CVD diamond coatings on SiC substrates. *Surf Coat Technol* 193:200–205
- Davis B, Dabrow D, Ju LC, Li AH, Xu CY, Huang Y (2017) Study of Chip Morphology and Chip Formation Mechanism During Machining of Magnesium-Based Metal Matrix Composites. *J Manuf Sci Eng* 139:091008–1
- Fowler PA, Hughes JM, Elias RM (2006) Biocomposites: technology, environmental credentials and market forces. *J Sci Food Agr* 86:1781–1789
- Gao YF, Ge PQ, Zhang L, Bi WB (2019) Material removal and surface generation mechanisms in diamond wire sawing of silicon crystal. *Mat Sci Semicon Proc* 103:104642
- Guo XL, Ekevad M, Marklund B, Li RR, Cao PX, Grönlund A (2014) Cutting forces and chip morphology during wood plastic composites orthogonal cutting. *BioResources* 9:2090–2106

- Guo XL, Li RR, Cao PX, Ekevad M, Cristovao L, Marklund B, Gronlund A (2015) Effect of average chip thickness and cutting speed on cutting forces and surface roughness during peripheral up milling of wood flour/polyvinyl chloride composite. *Wood Res* 60:147–156
- Kilinc K, Kanbur Y, Tayfun U (2019) Mechanical, thermo-mechanical and water uptake performance of wood flour filled polyurethane elastomer eco-composites: influence of surface treatment of wood flour. *Holzforschung* 73:401–407. <https://doi.org/10.1515/hf-2018-0116>
- Komanduri R, Von Turkovich BF (1981) New observations on the mechanism of chip formation when machining titanium alloys. *Wear* 69:179–188. [https://doi.org/10.1016/0043-1648\(81\)90242-8](https://doi.org/10.1016/0043-1648(81)90242-8)
- Kuzu AT, Bakkal M (2016) The effect of cutting parameters and tool geometry on machinability of cotton-fiber reinforced polymer composites: cutting forces, burr formation, and chip morphology. *J Ind Text* 45:1364–1382
- Lin Z, Renneckar S (2011) Nanocomposite-based lignocellulosic fibers 2: layer-by-layer modification of wood fibers for reinforcement in thermoplastic composites. *Compos A Appl Sci Manuf* 42:84–91. <https://doi.org/10.1016/j.compositesa.2010.10.011>
- Madhavan V, Lipczynski G, Lane B, Whinton E (2015) Fiber orientation angle effects in machining of unidirectional CFRP laminated composites. *J Manuf Process* 20:431–442
- Nairn JA (2016) Numerical modelling of orthogonal cutting: application to woodworking with a bench plane. *Interface Focus* 6:ARTN20150110. <https://doi.org/10.1098/rsfs.2015.0110>
- Pelaez-Samaniego MR, Yadama V, Lowell E, Espinoza-Herrera R (2013) A review of wood thermal pre-treatments to improve wood composite properties. *Wood Sci Technol* 47:1285–1319. <https://doi.org/10.1007/s00226-013-0574-3>
- Saloni D, Buehlmann U, Lemaster RL (2011) Tool wear when cutting wood fiber-plastic composite materials. *For Prod J* 61:149–154
- Thibaut B (1988) Le processus de coupe du bois par déroulage. Thèse d'état, Université Montpellier (The process of cutting wood by peeling, PhD thesis, Montpellier University)
- Thibaut B, Denaud L, Collet R et al (2016) Wood machining with a focus on French research in the last 50 years. *Ann For Sci* 73:163–184
- Vyas A, Shaw MC (1999) Mechanics of saw-tooth chip formation in metal cutting. *J Manuf Sci Eng* 121:163–172. <https://doi.org/10.1115/1.2831200>
- Wei W, Li Y, Xue T et al (2018) The research progress of machining mechanisms in milling wood-based materials. *BioResources* 13:2139–2149. <https://doi.org/10.15376/biores.13.1.Wei>
- Wyeth DJ, Goli G, Atkins AG (2009) Fracture toughness, chip types and the mechanics of cutting wood: a review COST Action E35 2004–2008: Wood machining—micromechanics and fracture. *Holz-forschung* 63:168–180

**Publisher's Note** Springer Nature remains neutral with regard to jurisdictional claims in published maps and institutional affiliations.